4.3 RECENT DEVELOPMENT OF GLOBAL AND REGIONAL LOCAL ENSEMBLE TRANSFORM KALMAN FILTERS (LETKF) AT JMA

Takemasa Miyoshi[1*], Shozo Yamane[2], Yoshiaki Sato[1], Kohei Aranami[1], and Takeshi Enomoto[3]

[1] Numerical Prediction Division, Japan Meteorological Agency

[2] Chiba Institute of Science, and Frontier Research Center for Global Change, JAMSTEC

[3] Earth Simulator Center, JAMSTEC

1. INTRODUCTION

At the Numerical Prediction Division, Japan Meteorological Agency (NPD/JMA), a four-dimensional local ensemble transform Kalman filter (4D-LETKF or just LETKF hereafter, Hunt et al. 2004; Hunt 2005) is being developed since August 2005. Thus far, we have achieved working LETKF systems with three state-of-the-art models: AFES (AGCM for the Earth Simulator, Ohfuchi et al. 2004), GSM (JMA's operational Global Spectral Model), and NHM (a.k.a. MSM, JMA's operational nonhydrostatic Mesoscale Model). Here, recent progress of the developments with AFES, GSM, and NHM is outlined in section 2, 3, and 4, respectively.

2. AFES-LETKF

2.1 *Project Overview*

The AFES-LETKF project is a collaborative project among the NPD/JMA, Chiba Institute of Science (CIS), and Earth Simulator Center (ESC). The NPD/JMA, ESC, and CIS develop the LETKF, AFES, and the experimental system connecting the LETKF data assimilation and AFES forecast, respectively. The model resolution is chosen to be T159/L48, corresponding to the grid of 480x240x48.

The LETKF FORTRAN90 codes are based on the local ensemble Kalman filter (LEKF, Ott et al. 2002; 2004) codes by Miyoshi (2005), with MPI/OpenMP-parallelization and upgrading to LETKF. Miyoshi and Yamane (2006, "MY06" hereafter) described details of the first outcome of the AFES-LETKF, including the code development, perfect model experiments, and experiments with real observations. Here, MY06 is briefly reviewed in section 2.2, followed by a brief description of the recent progress of so-called ALERA (AFES-LETKF Experimental ReAnalysis) in section 2.3. Moreover, recently Miyoshi et al. (2006) took advantages of an intrinsic property of LETKF, i.e., not requiring local patches, to propose an efficient implementation of LETKF with the error covariance localized only by physical distances, which solves the problem of analysis discontinuities near the Poles. Miyoshi et al. (2006) is reviewed in section 2.4.

2.2 *Brief Review of Miyoshi and Yamane (2006)*

MY06 performed three kinds of data assimilation experiments: 1) perfect model experiments with regular observing network, 2) perfect model experiments with real observing network, and 3) experiments with real observations except satellite radiances. They investigated sensitivities of the analysis accuracy to the ensemble size and localization parameters. They also investigated computational cost. In this section, their main findings are briefly reviewed.

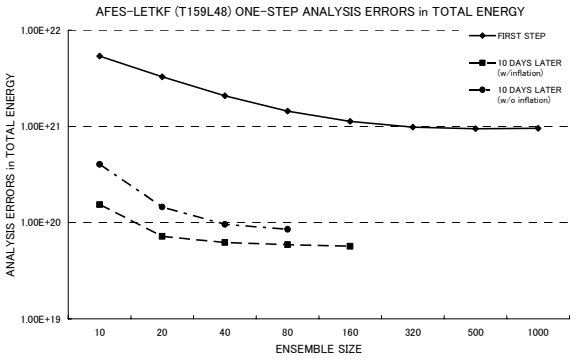

Figure 1. Analysis errors (total energy) at the first one-step analyses (solid line) and the analyses after 10-day cycles (broken lines) of LETKF with changing the ensemble size, adapted from Fig. 3 of MY06. Dashed and dash-dotted lines show the cases with and without covariance inflation, respectively. Due to the limited computational capability, 10-day cycle experiments have not been performed with more than 320 and 160 ensemble members for the cases with and without inflation, respectively.

* Corresponding author address: Takemasa Miyoshi, Numerical Prediction Division, Japan Meteorological Agency, 1-3-4 Otemachi, Chiyoda-ku, Tokyo 100-8122, Japan. E-mail: miyoshi@naps.kishou.go.jp

In the first perfect model experiments with regular observing network, MY06 investigated sensitivities and timing. Fig. 1 indicates the sensitivity to the ensemble size. The analysis errors are consistently decreased with increasing the ensemble size, but the decreasing ratio is smaller with larger ensemble sizes. Fig. 2 shows the sensitivity to the local patch parameters. There is non-negligible sensitivity, and too large localizations destroy the filter stability. Thus, once the ensemble size is fixed, tuning localization parameters is suggested. To explain the sensitivity, MY06 also investigated how the error covariance is localized with various localization parameters. The cross-covariance structure includes dynamical balance; they discussed that a severe localization does not destroy the balance. The figures showing the covariance (Figs. 6-9 in MY06) are not shown in this abstract. Timing is shown in Table 1. If we use the same number of computational nodes as the ensemble size, the computational time is less than 4 minutes. The acceleration ratio (Fig. 10 of MY06, not shown) indicates almost 99.99% parallelization ratio with more than 80 members. MY06 also investigated timing with various local patch sizes, indicating quadratic relationship (Fig. 11 of MY06, not shown).

Here, we skip the second perfect model experiments and summarize the results with real observations. The AFES-LETKF analysis field looks almost identical to the JMA operational analysis; most areas show the difference less than 0.5 hPa in sea-level pressure (Fig. 15 of MY06, not shown). MY06 performed 48-hour forecast experiments and verified the forecast against own analyses. Fig. 3 shows the forecast verification results, indicating similar performances among our LETKF and operational analyses (T213/L40 JMA operational analysis and T62/L28 NCEP/NCAR reanalysis). Note that operational analyses assimilate satellite radiances, which are known to have significant positive impacts in the SH. Overall in the 48-hour forecast verification, LETKF shows as good performance as the operational analyses.

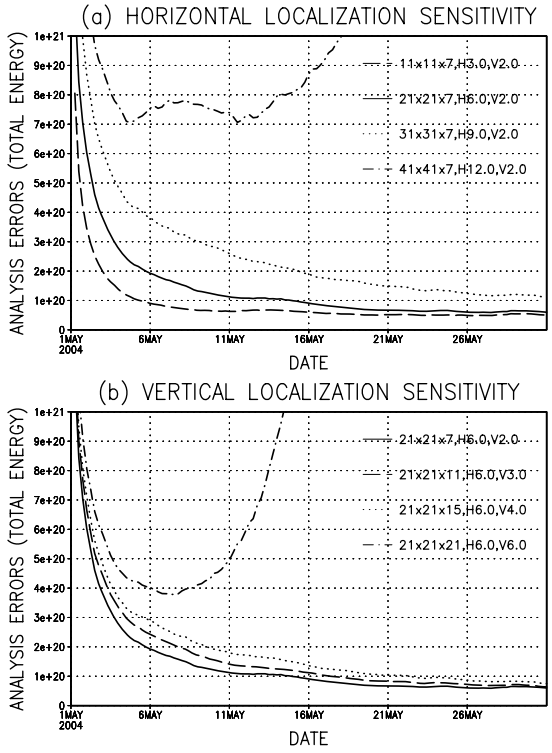

Figure 2. Time series of analysis errors (total energy) of LETKF with 40 ensemble members with various horizontal (a) and vertical (b) localization parameters, adapted from Fig. 5 of MY06. Solid lines in (a) and (b) show the case of 21x21x7 local patch with 6.0-grid horizontal and 2.0-grid vertical localization (denoted by 21x21x7, H6.0, V2.0). The line legends show localization parameters for each line.

Table 1. Timing (sec.) of LETKF on the Earth Simulator, adapted from Table 1 of MY06.

Ensemble size	5 nodes	10 nodes	20 nodes	40 nodes	80 nodes
10	382	195	115	67	47
20	714	360	197	107	66
40	1389	708	360	189	112
80		1583	824	413	220
160				1205	626

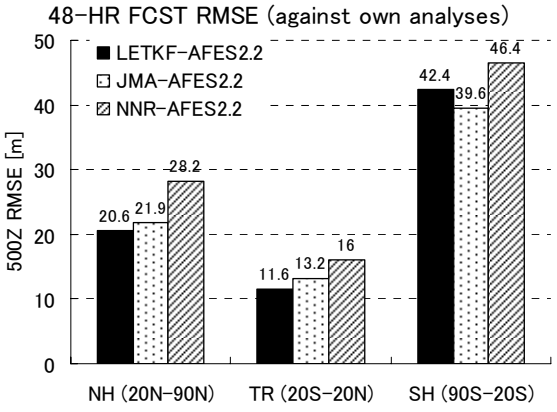

Figure 3. 48-hour forecast RMS errors of 500 hPa height (m), averaged over 16 days initialized on August 11 through August 26 in 2004, adapted from Fig. 16 of MY06. The errors are defined as the differences between 48-hour forecasts and the own analyses. JMA-AFES2.2 indicates that JMA operational analyses are forecasted by AFES2.2, and similarly for NNR (NCEP/NCAR reanalysis) and LETKF.

2.3 *Experimental Ensemble Reanalysis: ALERA*

Based on the successful implementation and preliminary tests by MY06, we have been performing longer-term data assimilation cycle experiments with real observations except satellite radiances; the project is called “ALERA”, standing for AFES-LETKF Experimental ReAnalysis. The ensemble size is fixed to be 40, and the experimental period is from May 2005 towards today as long as computational resources are available.

Since in general there is no guarantee that the ensemble Kalman filter (EnKF) is stable for a long period, the primary purpose of ALERA is to investigate the long-term stability of the AFES-LETKF system. Fig. 4 shows time series over 1 year of the analysis ensemble spreads and analysis differences between AFES-LETKF and NCEP/NCAR reanalysis. The AFES-LETKF performs stably for over 1 year. The discontinuity after the initial one month is due to the system upgrade, where we began to apply the vertical localization for surface pressure observations. If the discontinuity is ignored, AFES-LETKF has an about 1-week spin-up period. After the spin-up, the analysis differences are quite stable. We see some seasonal variations: larger analysis differences in winter hemisphere, especially in the NH. However, spreads have smaller seasonal amplitudes.

ALERA contains huge amount of information: 40 analysis members every 6 hours. At an analysis time, Fig. 5 shows the spaghetti diagram of 500 hPa height fields. ALERA contains this kind of map every 6 hours for all variables at all vertical levels. Therefore, it is important to analyze the products more in detail, which is now in progress.

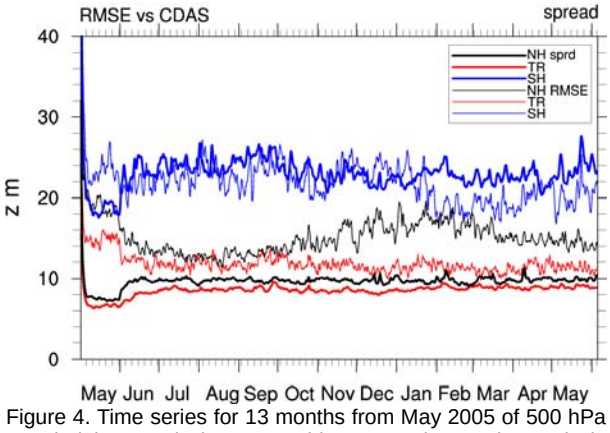

Figure 4. Time series for 13 months from May 2005 of 500 hPa height analysis ensemble spreads and analysis differences between AFES-LETKF and NCEP/NCAR reanalysis (CDAS) in each region.

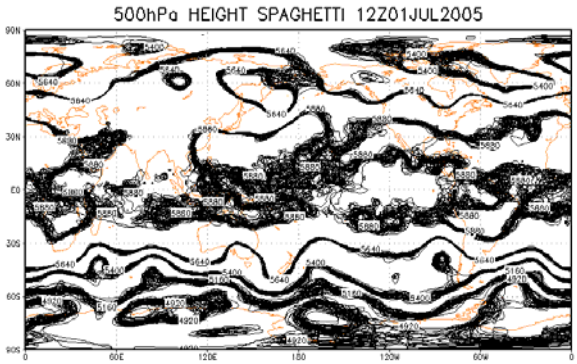

Figure 5. Spaghetti diagram of 500 hPa height (m) for the ALERA analysis ensemble on 12Z July 1, 2005.

2.4 *LETKF Implementation with Error Covariance Localization only by Physical Distances*

Although the LEKF requires local patches, not requiring local patches is an intrinsic property of the LETKF. Miyoshi et al. (2006, “MYE06” hereafter) took advantages of the property to propose an efficient LETKF implementation with the error covariance localized only by physical distances to solve the problem of analysis discontinuities in the Polar Regions. As shown in the top panel of Fig. 6, the analysis ensemble spread by MY06 shows rectangular shapes corresponding to local patches. We see discontinuities at the edges of the local patch, especially near the Poles, which is not preferable. If we drop the local patches and localize the error covariance only by physical distances, such discontinuities disappear completely, as shown in the bottom panel of Fig. 6. The latter looks much more natural. In fact, the analysis accuracy is improved in the Polar Regions (Fig. 7).

Now that the error covariance is localized only by physical distances, the number of localization tuning parameters is reduced to be just horizontal and vertical physical length scales. This is a major advantage considering the tuning process. However, due to the additional computations of accurate physical distances, it is essential to optimize the algorithm. An efficient sorting algorithm has been implemented to optimize the searching process of observations and to minimize the distance computations. Overall, the computation is accelerated by about three times. The details of the efficient implementation are described in MYE06. The new implementation without local patches would be our future choice.

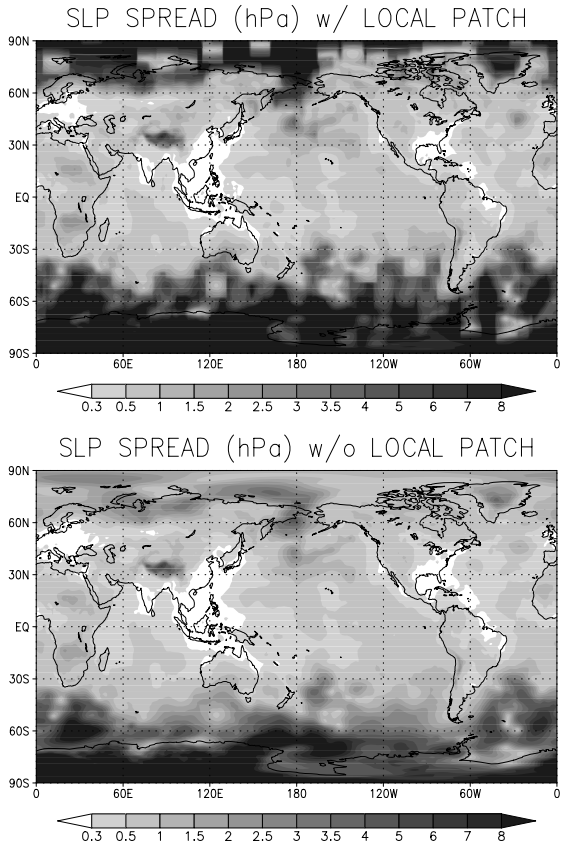

Figure 6. Ensemble spread of sea-level pressure (hPa) on 00Z August 1, 2004 (first analysis) with the original LETKF by MY06 (top) and the modified LETKF without local patches (bottom), both assimilating the same observations (adapted from Fig. 2 of MYE06).

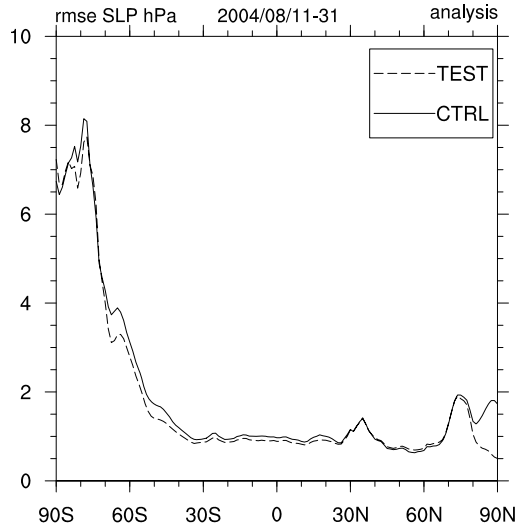

Figure 7. Zonal mean of the root mean square differences against JMA operational analysis of sea-level pressure (hPa) for the original (solid, with local patches) and new (dashed, without local patches) versions of LETKF, temporally averaged for 21 days from 11 to 31 August 2004 (adapted from Fig. 5 of MYE06).

3. GSM-LETKF

3.1 *Project Overview*

Based on results by MY06 on the Earth Simulator, LETKF has been developed with JMA operational global model (GSM) and adapted into JMA's operational experimental system known as NAPEX (Numerical Analysis and Prediction EXperiment system, originally developed by K. Onogi and maintained by NPD). The NAPEX includes major operational global NWP components at JMA; for example, the observational quality control procedure is embedded. The model resolution is chosen to be TL159/L40, the same as the operational EPS. At this moment, three kinds of preliminary experiments have been completed: 1) 20-member LETKF without satellite radiances, 2) 20-member LETKF with satellite radiances, 3) 50-member LETKF with satellite radiances. These results clarify the effects by assimilating satellite radiances and increasing the ensemble size from 20 to 50. Using the first two experiments with 20 members, Miyoshi and Sato (2006, "MS06" hereafter) investigated the effects by satellite radiances. MS06 is reviewed in section 3.2. The results of the 50-member experiment are described in section 3.3.

3.2 *Brief Review of Miyoshi and Sato (2006)*

It is not straightforward how to assimilate satellite radiances within EnKF. MS06 found that assimilating satellite radiances without localizing the vertical error covariance resulted in large analysis errors. Increasing the covariance inflation reduces the analysis errors, which suggests that we extract too much information from satellite radiances due to spurious covariance components among vertically distant points. In fact, the surface pressure analysis ensemble spread is greatly reduced by satellite radiances, although we do not assimilate satellite channels sensitive to surface pressure.

Therefore, MS06 proposed a way to localize the vertical error covariance to reduce sampling errors. Precisely, MS06 normalized the observational sensitivity function to be used as a localization weighting function. Namely, the levels at which a specific satellite channel is sensitive have smaller localization weights in assimilating the channel, and vice versa. This significantly contributes to assimilate satellite radiances effectively and to keep the analysis ensemble spread to

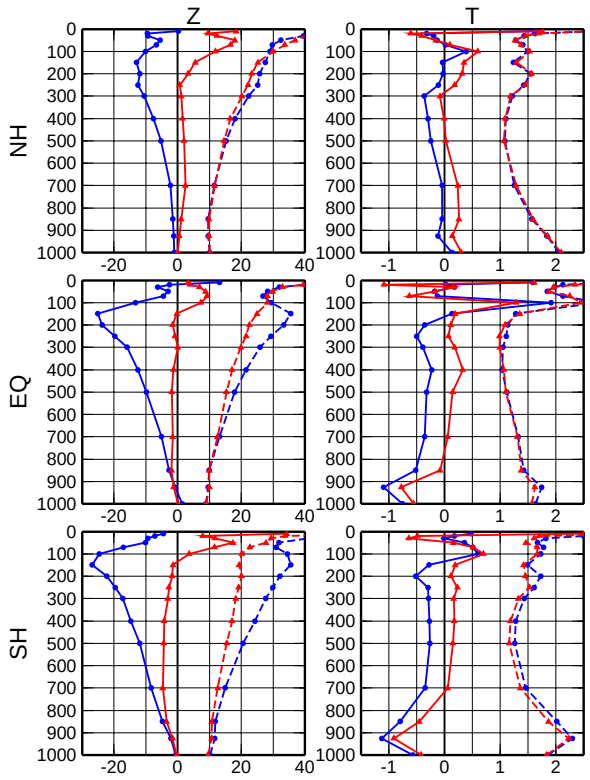

Figure 8. Analysis errors of height (m, left) and temperature (K, right) verified against radiosonde observations in each area for the cases with (red) and without (blue) satellite radiances, temporally averaged over 31 days in August 2004 (adapted from Fig. 5 of MS06). Solid and dashed lines indicate the bias and RMS errors, respectively.

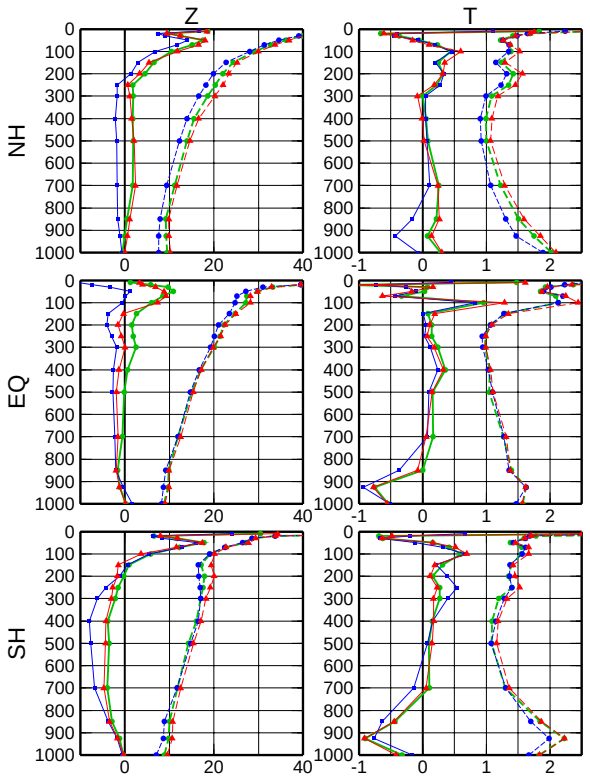

Figure 9. Similarly to Fig.8 but for the cases of the LETKF with 20 members (red), LETKF with 50 members (green), and the operational 4D-Var (blue).

be an appropriate size. Fig. 8 shows the analysis errors verified against radiosonde observations, where we see significantly smaller errors by satellite radiances. MS06 performed 9-day forecast experiments, which also indicate advantages of assimilating satellite radiances (cf. Fig. 6 of MS06).

3.3 *Results of 50-member Experiment*

After MS06 found an appropriate way to assimilate satellite radiances, the ensemble size was increased to 50 to compare with the operational 4D-Var analysis (TL319/L40 outer and T106/L40 (equivalent to TL159/L40) inner resolutions). Fig. 9 shows the analysis errors verified against radiosondes, indicating that 50-member LETKF outperforms 20-member LETKF. Still, generally 4D-Var outperforms LETKF even with 50 members. The difference between LETKF and 4D-Var is smaller in the SH than in the NH; LETKF is advantageous in data-poor regions. One of the parts where LETKF outperforms 4D-Var is around the mid-

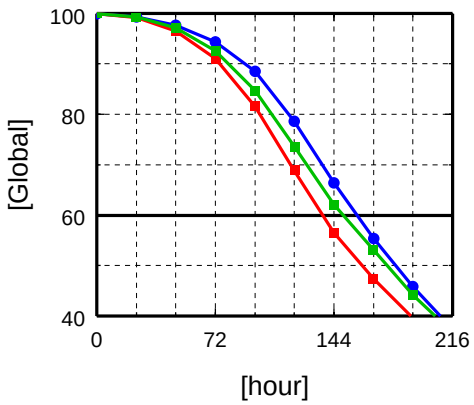

Figure 10. 9-day forecast anomaly correlations (%) of 500 hPa height for the cases of the LETKF with 20 members (red), LETKF with 50 members (green), and operational 4D-Var (blue).

troposphere (500 – 300 hPa) in the SH. It is noted that we see larger improvements by increasing the ensemble size in middle to upper troposphere, whereas the improvements are small at lower levels. This is not the case with what Anderson et al. reported (Khare, pers. comm.); EnKF is advantageous at lower levels with their 80-member EAKF (ensemble adjustment Kalman filter, Anderson 2000) applied to T85 CAM (NCAR climate

community model) compared with the T254 NCEP GDAS (operational 3D-Var global data assimilation). The weakness of our LETKF at lower levels would be partly due to the vertical localization; we force zero error covariance beyond 3 vertical levels, so that near the surface, where the model resolution is dense, we might not extract enough information from observations.

9-day forecast experiments are performed. Fig. 10 shows 500 hPa height forecast anomaly correlations, where we see large improvements by increasing the ensemble size from 20 to 50. However, still 4D-Var clearly outperforms LETKF.

4. NHM-LETKF

4.1 *Project Overview*

JMA is operating a nonhydrostatic mesoscale model (NHM or a.k.a. MSM) with 5-km grid spacing. To initialize the NHM, hydrostatic regional 4D-Var with 10-km outer and 20-km inner grid spacing is in operations. Since EnKF is generally applicable to any dynamical models with minimal modifications, LETKF is applied to NHM. Miyoshi and Aranami (2006, "MA06" hereafter) developed the LETKF system and tested with a perfect model scenario. Following the successful investigations by MA06, real observations are assimilated. Here, MA06 is overviewed in section 4.2, followed by the preliminary results assimilating real observations in section 4.3.

4.2 *Brief Review of Miyoshi and Aranami (2006)*

MA06 developed the LETKF system considering the differences in boundary conditions and prognostic variables (3-dimensional pressure and water-related quantities). They performed 10-member LETKF with NHM at a 5-km grid spacing under the perfect model assumption. The model domain is almost a square of about 300 km by 300 km with 65x63x50 grid points. The model parameters are chosen to be the same as the ones used in operations. Horizontal winds (1.0 m/s), temperature (1.0 K), and relative humidity (10 %) are observed every 2x2x2 grid points (parenthesis indicates observational error standard deviations). Surface pressure (1.0 hPa) and precipitation rate (1.0 mm/hr) are also observed at surface every 2x2 grid points. The temporal frequency of observations is every 10 minutes. The data assimilation cycle interval is 1 hour, thus the 4-dimensional assimilation is performed with 6 time

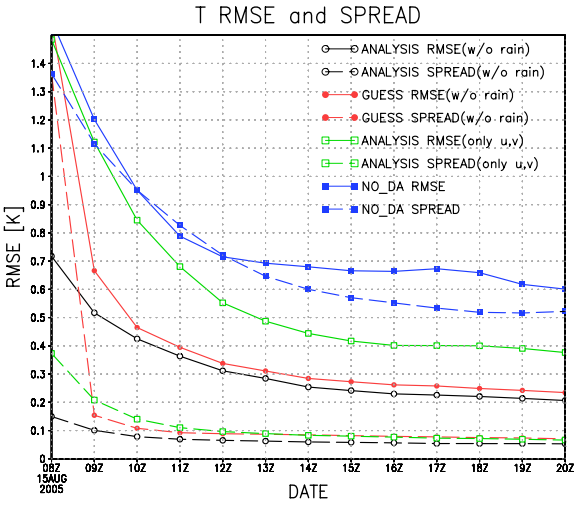

Figure 11. Time series of temperature RMSE (K, solid lines) and ensemble spread (K, broken lines), averaged horizontally except boundary points and vertically from the 2nd to 40th levels. Black, and red lines show analysis and first guess in the case assimilating all observing elements except precipitation rate (w/o rain), adapted from Fig. 2 of MA06. Green lines show the case assimilating only wind observations (only u, v). For comparison, RMSE and ensemble spread in the case without data assimilation are shown in blue lines. Solid and broken lines indicate RMSE and spread, respectively.

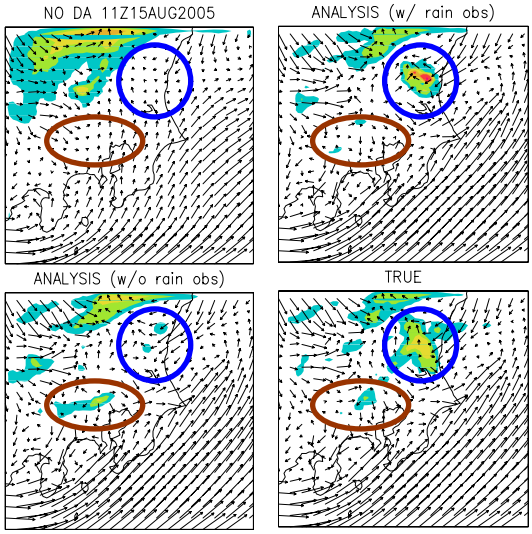

Figure 12. Precipitation pattern and wind vectors at 11Z, after 4 analysis steps, adapted from Fig. 4 of MA06. Each panel indicates the cases with no data assimilation (top left), LETKF without precipitation assimilation (bottom left), LETKF with precipitation assimilation (top right), and the true state (bottom left).

slots. 10% multiplicative spread inflation (21% covariance inflation) is applied.

Fig. 11 shows time series of the temperature analysis root mean square errors (RMSE), where they are decreasing even without data assimilation since the

perfect boundary conditions are given. Still, LETKF indicates clear advantages. Spreads are larger in the first guess than in the analysis, which indicates the LETKF ensemble perturbations are actually growing in an hour. Even assimilating only winds, we see significant error reduction. Assimilating precipitation causes slight negative impacts (not shown).

Fig. 12 shows precipitation patterns and wind vectors at 11Z, after four data assimilation steps. The true state indicates strong precipitation in the blue-circled area, where we see no sign of precipitation in the case without data assimilation. Assimilation all observed data (including precipitation) recovers this precipitation, although without precipitation assimilation, it is not reproduced well. On the contrary, the convective cell in the blown circle is better captured in the case without precipitation assimilation. In fact, the convective system is already damped in the case with precipitation assimilation, where we see diverging flow near surface. The timing was a little earlier for the convective system in the case with precipitation assimilation.

In summary, the NHM-LETKF system works appropriately with NHM containing explicit cloud microphysics. Assimilating precipitation has negative impacts in general, but positive impacts are observed for some specific precipitation systems.

4.3 *Assimilation of Real Observations*

After the successful preliminary investigation by MA06, real observations used in JMA's operational mesoscale analysis are assimilated with NHM-LETKF. The model domain is extended to be the same as the JMA operational mesoscale system (about 3600km x 2900km). The resolution is reduced to be 20-km grid spacing with 181x145x50 grid points. The ensemble size is chosen to be 20. The data assimilation cycle begins on June 25, 2004.

Fig. 13 shows 6-hour forecast fields (i.e., first guess) of the NHM-LETKF and JMA operational mesoscale NWP systems. Although NHM-LETKF indicates a little higher pressure, the position of the low pressure system and precipitation pattern shows good agreements.

Fig. 14 shows analysis ensemble spreads after the first analysis step and a few week cycle processes. Since a large number of observations are available over Japan, the area with small spreads indicates the shape of Japan after the first analysis step. Due to the fixed boundary conditions for all ensemble members, spreads are artificially small near the boundaries, especially about 20 grids (400 km) which corresponds to the damping area. Still, we see large spreads beyond 7 m/s in the region; the errors are actually growing and not damped by the fixed boundaries. The ensemble spreads vary dynamically to show flow-dependent behaviors. The stable LETKF performance would explain that the error growth inside the region is not significantly affected by the fixed boundary conditions.

5. SUMMARY AND DISCUSSION

LETKF has been applied to three state-of-the-art models: AFES, GSM and NHM. It has been shown that LETKF works appropriately with the three models with real observations. Since LETKF analyzes the analysis errors, it would provide additional information that has not been available before. The new information has a lot of potential usages such as supporting targeted observations. Although there are remaining problems including precipitation assimilation, it is worth continuing

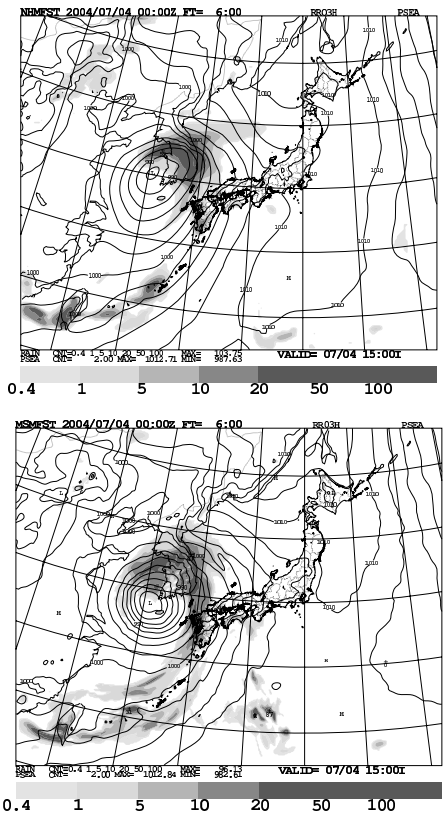

Figure 13. 3-hour accumulated precipitation (mm/hr, shades) and sea-level pressure (contour) of NHM-LETKF 6-hour forecast ensemble mean (top) and JMA operational mesoscale 6-hour forecast (bottom) valid on 06Z July 4, 2004.

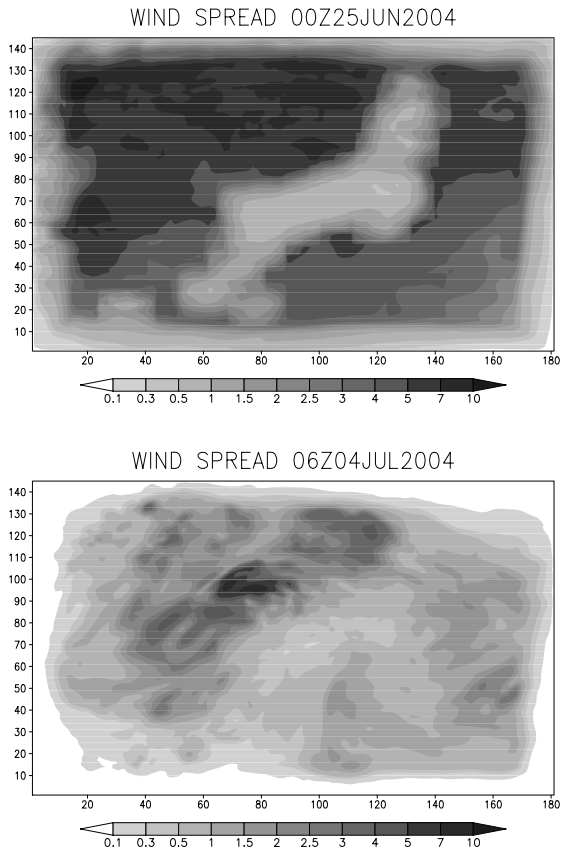

Figure 14. Horizontal pattern of the analysis ensemble spreads of wind speed (m/s) at the 21st vertical level, after first analysis step (00Z June 25, 2004, top) and a few week cycle processes (06Z July 4, 2004, bottom).

the development towards operations.

After the successful preliminary investigations, we are now at the stage to improve the performance to be compared to the operational system. The operational EnKF system with perturbed observations by Houtekamer et al. (2005) has been proven to be comparable to the operational 4D-Var at CMC (Canadian Meteorological Centre). Whitaker et al. (2006) reported EnKF with 100 members is comparable to operational T254 NCEP GDAS (operational 3D-Var). Anderson et al. (Khare, pers. comm.) also reported that their EAKF with T85 CAM was comparable to T254 NCEP GDAS. These pioneering works greatly encourage us that we could improve our LETKF to be comparable to the operational 4D-Var at JMA. If LETKF is proven to be at least comparable to 4D-Var, it would be the choice for the future operational system. LETKF is much more efficient to maintain, since it does not require the linearized model and its adjoint. Moreover, it is essentially model independent, so that we could use the same LETKF for both global and mesoscale data assimilation and ensemble prediction systems.

Based on the pioneering works described above, our future directions to improve the LETKF to a comparable level with the operational 4D-Var is to increase the ensemble size up to about 100, to tune the error covariance localization and inflation, and possibly to increase the model resolution. The new implementation of LETKF without local patches described in section 2.4 would play an important role in tuning localization. We also plan to investigate the performance of the LETKF as an ensemble prediction system (EPS), so that it could be applied to the operational EPS at first. To apply in operations, it is important to find that the LETKF system outperforms the current operational systems, which is very challenging as shown in the present study.

ACKNOWLEDGEMENTS

We thank members of the chaos/weather group of the University of Maryland, especially Prof. Eugenia Kalnay for fruitful discussions. We also thank Dr. Wataru Ohfuchi of ESC and Dr. Tadashi Tsuyuki, Yoshiaki Takeuchi, Yuzo Yotsuya, and Ko Koizumi of NPD/JMA for kind support for the LETKF projects. The AFES-LETKF experiments have been performed on the Earth Simulator under support of JAMSTEC.

REFERENCES

Anderson, J. L., 2001: An ensemble adjustment Kalman filter for data assimilation. *Mon. Wea. Rev.*, **129**, 2884-2903.

Houtekamer, P. L., H. L. Mitchell, G. Pellerin, M. Buehner, M. Charron, L. Spacek, and B. Hansen, 2005: Atmospheric Data Assimilation with an Ensemble Kalman Filter: Results with Real Observations. *Mon. Wea. Rev.*, **133**, 604-620.

Hunt, B. R., E. Kalnay, E. J. Kostelich, E. Ott, D. J. Patil, T. Sauer, I. Szunyogh, J. A. Yorke, and A. V. Zimin, 2004: Four-dimensional ensemble Kalman filtering. *Tellus*, **56A**, 273-277.

Hunt, B. R., 2005: Efficient Data Assimilation for Spatiotemporal Chaos: a Local Ensemble Transform Kalman Filter. arXiv:physics/0511236v1, 25pp.

Miyoshi, T., 2005: Ensemble Kalman filter experiments with a primitive-equation global model. Ph.D. dissertation, University of Maryland, 197pp.

Miyoshi, T. and K. Aranami, 2006: Applying a Four-dimensional Local Ensemble Transform Kalman Filter (4D-LETKF) to the JMA Nonhydrostatic Model (NHM), *SOLA*, **2**, 128-131.

Miyoshi, T. and Y. Sato, 2006: A vertical covariance localization technique to assimilate satellite radiances with an ensemble Kalman filter. *Mon. Wea. Rev.*, submitted.

Miyoshi, T. and S. Yamane, 2006: Local ensemble transform Kalman filtering with an AGCM at a T159/L48 resolution. *Mon. Wea. Rev.*, submitted.

Miyoshi, T., S. Yamane, and T. Enomoto, 2006: Localizing the error covariance by physical distances within a local ensemble transform Kalman filter. *Tellus*, submitted.

Ohfuchi, W., H. Nakamura, M. K. Yoshioka, T. Enomoto, K. Takaya, X. Peng, S. Yamane, T. Nishimura, Y. Kurihara, and K. Ninomiya, 2004: 10-km mesh meso-scale resolving simulations of the global atmosphere on the Earth Simulator: Preliminary outcomes of AFES (AGCM for the Earth Simulator). *J. Earth Simulator*, **1**, 8-34.

Ott, E., B. R. Hunt, I. Szunyogh, M. Corazza, E. Kalnay, D. J. Patil, J. A. Yorke, A. V. Zimin, and E. J. Kostelich, 2002: Exploiting Local Low Dimensionality of the Atmospheric Dynamics for Efficient Ensemble Kalman Filtering. arXiv:physics/0203058v3.

Ott, E., B. R. Hunt, I. Szunyogh, A. V. Zimin, E. J. Kostelich, M. Corazza, E. Kalnay, D. J. Patil, and J. A. Yorke, 2004: A local ensemble Kalman filter for atmospheric data assimilation. *Tellus*, **56A**, 415-428.

Whitaker, J. S., T. M. Hamill, X. Wei, Y. Song and Z. Toth, 2006: Ensemble Data Assimilation with the NCEP Global Forecast System. *Mon. Wea. Rev.*, submitted.